ORIGINAL ARTICLE

lajss.org© Latin American Journal of Solids and Structures

www.lajss.org

Interaction of double parallel cracks located on a hollow cylinder

Omar Mohammed Al-Moayed[a]*, Al Emran Ismail[b], Ali Kamil Kareem[c], Saifulnizan Jamian[b], Gabriel de Castro Coêlho[d]

[a]Renewable Energy Research Center, University of Anbar, Ramadi, Iraq. E-mail: omar.m.f@uoanbar.edu.iq
[b]Faculty of Mechanical and Manufacturing Engineering, University Tun Hussein Onn Malaysia, Batu Pahat, 86400, Malaysia. E-mail: emran@uthm.edu.my, saifulnz@uthm.edu.my
[c]Department of Biomedical Engineering, Al-Mustaqbal University College, Babylon, Iraq. E-mail: ali.kamil.kareem@uomus.edu.iq
[d]Department of Mechanical Engineering, Universidade Federal de Campina Grande, Campina Grande 58429-900, Brasil. E-mail: gabriel.coelho@estudante.ufcg.edu.br

* Corresponding author

https://doi.org/10.1590/1679-78257786

Abstract

Due to the extensive usage in the industry, the structural integrity of hollow cylinders is seen as a critical goal for stakeholders. Fracture is the most common failure mode for cylinders, which occurs due to crack propagation. Cracks can be found in single or multiple forms; when numerous, crack interaction occurs, which can exacerbate pressures beyond the material's resistance. This work uses Ansys software to examine double parallel interacting surface cracks on a hollow cylinder. The stress intensity factor (SIF) was used to describe the driving force that was used to characterize crack interaction for various crack geometries. To conduct extensive research, this study evaluated a wide range of crack aspect ratios as well as the relative depth of the crack. The findings of this study indicated that the shielding effect demonstrated parallel crack interaction. In addition, an empirical mathematical approach for predicting SIFs for double parallel cracks via single crack SIFs has been developed. The validation of the proposed model using performance evaluation metrics revealed an acceptable rate of error of less than 5%.

Keywords

Crack interaction, Circumferential crack, hollow cylinder, SIFs, Parallel cracks, Ansys.

Graphical Abstract

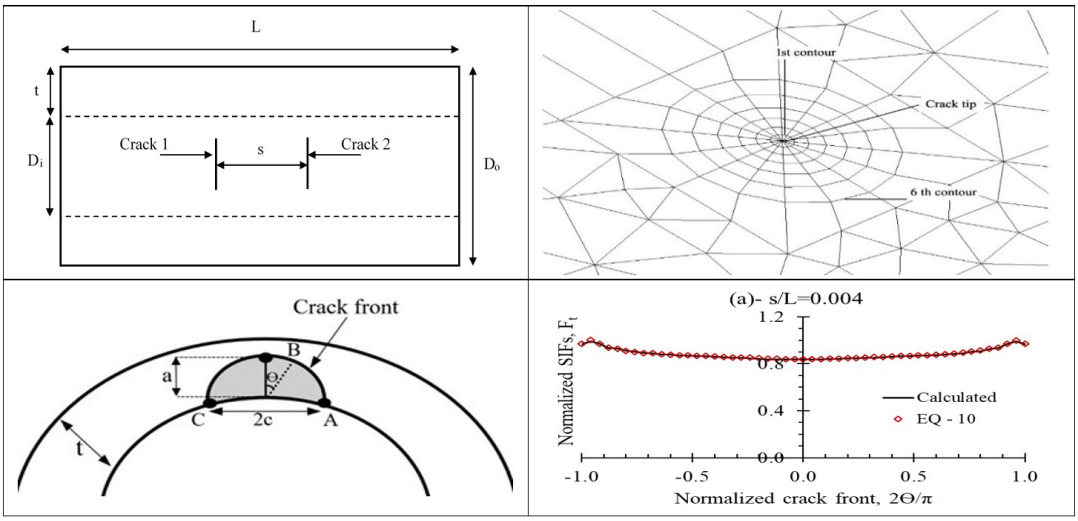

Received: July 30, 2023. In revised form: September 20, 2023. Accepted: October 20, 2023. Available online: October 26, 2023
https://doi.org/10.1590/1679-78257786

Latin American Journal of Solids and Structures. ISSN 1679-7825. Copyright © 2023. This is an Open Access article distributed under the terms of the Creative Commons Attribution License, which permits unrestricted use, distribution, and reproduction in any medium, provided the original work is properly cited.

1 INTRODUCTION

Largely, cylinders (solid or hollow) mechanical components are used in a wide range of industries, particularly aerospace, offshore, pipeline, and pressure vessels. Their many uses originate from the outstanding combination of strength and weight they provide. Cylindrical structures are essential components in pressure vessels, pipelines, storage tanks, and structural frameworks that must operate under extreme conditions. Nevertheless, the vulnerability of cylinders to failure is still an increasing apprehension in the practical engineering field (Li and Yang 2012).

A review of cylinder failures in service found that the majority of failures are of the fracture category, which means failure occurs due to the growth of a flaw or crack leading to cylinder collapse (Marshall 2001). In the literature, several studies tried to solve the problem of multiple interacting surface cracks. The diversity of these studies was found to be in different aspects such as the examined body, crack shape and geometry, crack location, orientation and configuration, and loading type. Furthermore, the term examined body clarifies whether the examined body is a plate or cylinder, in the case of a cylinder if it's solid or hollow (thick and thin). On the other hand, the crack shape is characterized as straight, slender, semi-elliptical, circular, and transverse, while crack geometry is defined in terms of crack depth and length. Also, the variety in the crack location is identified by the position of the crack on the outside or inner surface of the examined cylinder. Similarly, the orientation of the crack explains if the crack is axial, circumferential, or inclined. Besides, the crack configuration describes how the cracks are organized within the examined structure, this includes various crack configurations such as edge, embedded, colinear, coplanar, non-coplanar, and parallel.

Multiple crack interaction in plates has been investigated widely in the literature. Previously, (Jiang, Petit, and Bezine 1992) investigated the interaction of two unequal parallel edges and central cracks in a finite-width plate subjected to remote tensile loading using the Finite Element Method (FEM). The SIFs were the driving force; therefore, the distribution of the SIFs along the crack front was calculated and presented in the form of nondimensional SIFs. Due to the presence of the interaction phenomenon, the stress fields close to the crack tips are relaxed; thus, SIFs at both crack tips are shielded. In addition, (Chat Guozhong, Kangda, and Dongdi 1996) researched and analyzed the interaction effect of two coplanar elliptical cracks with similar and dissimilar crack sizes embedded in a finite thickness plate beneath uniform tension. Numerical analyses were conducted by the hybrid boundary element method (HBEM). Based on the outcomes of this study, the interaction effect in parallel cracks was found to be stronger than that of coplanar cracks. In coplanar cracks, the highest value of interaction is attained for two circular equal cracks, while for the parallel cracks, the highest interaction effect is achieved for two dissimilar cracks. Besides, (Abbaszadeh Bidokhti and Shahani 2015) examined the influence of crack interaction in a plate with two non-aligned cracks utilizing the Extended Finite Element Method (X-FEM). The impact of crack offsets and distances on each mode I and II SIFs were assessed. Based on the results, the study proposed modified combination rules. Also, (Guangwei et al. 1999) studied the problem of two parallel interacting cracks located centrally in a plate. This study employed the Singular Quasi-Compatible Finite Element (SQCE). The influence coefficients of different separation distances between cracks were produced in a tabulated form.

While The Fractal-like Finite Element Method (FFEM) was selected to research the interaction behavior of multiple penny-shaped cracks located on a solid cylinder subjected to tensile loading (Tsang, Oyadiji, and Leung 2003), the SIFs results revealed that the strength of a multiple-cracked structure is greater than that of a single crack underneath similar circumstances. Also, small distances between cracks lead to small SIFs, which point to high structural strength in case of multiple cracks. Instead, concerning multiple cracks in a hollow cylinder, (Kirkhope, Bell, and Kirkhope 1991) evaluated mode I SIFs for single and multiple numbers of axial surface cracks located on a pressurized thick hollow cylinder. The FEM has been exploited to attain the SIFs. This study intended to correlate the FE results for single and multiple crack cases, which were then used to derive empirical expressions for mode I SIFs at the deepest and surface points on the crack front. Based on the findings, closed-form equations have been introduced to quantify the impacts of crack shape and depth on the SIFs for single and arrays of similar cracks at the inner surface of a thick hollow cylinder. In order to determine the interaction behavior of two coplanar longitudinal cracks positioned in a cylinder, FEA accompanied by Fracture Mechanics analysis was conducted (Kim and Lo 1995). This study has taken into account the stress field close to the crack tip as a key parameter for the crack interaction. Therefore, in FEA, J-integral, as well as the stress field, were evaluated to determine the interaction of the fracture driving force. Based on the results, an equivalent crack driving force was introduced to perform more practical assessments of the crack interaction problem. Also, the interaction between longitudinal external and internal cracks located in a cylindrical pressure vessel was investigated (Guozhong et al. 2004). The HBEM was employed to perform the numerical analysis to obtain the SIFs for a broad assortment of crack and cylinder geometry. The results showed that, due to internal pressure loading, internal cracks revealed higher SIFs compared to external cracks. By the means of crack interaction, the cracks being deeper, the more critical they are, which could lead to crack propagation. In addition, (Y. M. Zhang et al. 2015) and (Y. Zhang, Fan, and Xiao 2016) performed 3-D FEA on a circumferentially cracked hollow cylinder with one semi-elliptical surface crack and an elliptical embedded crack by Crack-Tip Opening Displacement (CTOD). The 3-D

elastic-plastic examination has been performed for the interaction behaviors of two collinear cracks. The impact of each crack orientation, deviation distance, and internal pressure on the cracking performance is examined. The results of this study indicated that for different examined loading conditions, the most severe fracture response can be generated by tension combined with high-level internal pressure. Likewise, a new strain-based CTOD prediction technique is proposed to evaluate the fracture behavior of a cracked pipe with two interacting collinear flaws. Moreover, the impact of crack interaction on the Limit Load (LL) was obtained via FEA (Kamaya 2011). In this study, two equal circumferential surface cracks were positioned on the internal and external surfaces of a pipe subjected to uniform tensile stress. The primary concern was on the change in limit load reliant on the change of configurations of the crack along with the pipe. The results revealed that the level of interaction relies on the separation distance between cracks as well as the geometrical parameters of the crack and the cylinder. Depending on the study outcome and the analysis, a new criterion for the combination rule for the limit load is proposed.

It can be concluded that the crack configurations and geometry played a major role in the examination of crack interaction, which can interpret the diversity of the studies in the literature. Therefore, in this paper, SIFs for double circumferential parallel cracks located in a hollow cylinder are determined. Moreover, SIFs have been nominated to demonstrate the driving force of the crack interaction, by using SIFs the interaction behaviour can be described. In addition, a regression technique was utilized to correlate between SIFs of single and double cracks. A wide range of crack aspect ratios (crack depth, a / half crack length, c) was used from 0.4 to 1.2, and the relative depth of the crack ratio (crack depth, a / cylinder thickness, t) equal to 0.2, 0.5, and 0.8. The parallel crack configuration was examined first on the external surface of the cylinder, and then on the internal surface under different types of loading, tension, bending, and mixed-mode. It should be noted that in this study two hollow cylinder types were used, thick and thin, depending on wall thickness to internal diameter ratio.

2 PROBLEM LAYOUT

In this section, the description of the parallel crack configuration along with the exploited cylinder geometry is introduced. A hollow thick and thin cylinder with geometries presented in Table 1 is used to explore the problem of double-interacted parallel cracks.

The parallel configuration contains two identical circumferential cracks positioned either on the outer or inner surface of the hollow cylinder, separately. The cracks are named crack-1 and crack-2; cracks are separated by a horizontal distance s, as shown in Figure 1. It should be noted that s, was assumed based on the API 579-1 standard (API 2016), where the standard stated that the maximum allowable separation distance for interaction between the cracks is 13mm. Therefore, s was taken beyond the specified limit to investigate the influence of s on the interaction. Consequently, s = 3mm, 6mm, 12mm, and 24mm, and then s has been normalized, thus, s/L is taken to be 0.004, 0.008, 0.016, and 0.032.

Table 1. Thick and thin cylinder geometries

Parameter	Thick cylinder	Thin cylinder
Internal diameter, D_i	200mm	200mm
Outer diameter, D_o	250mm	220mm
Wall-thickness, t	25mm	10mm
Length, L	750mm	750mm
t/R_i	0.25	0.10

On the other hand, in order to perform a broad investigation range, the a/c ratio is taken to vary from 0.4 to 1.2. This range supports different crack shapes, such as slender and transverse shapes. Also, a/t taken equal to 0.2, 0.5, and 0.8, where these three values ensure examining shallow as well as deep cracks. Table 2 provides the characteristics of the structural steel material that has been used in this study.

Table 2. Material properties of structural steel

Property	Value
Young's modulus	200 GPa
Poisson's ratio	0.3
Tensile yield strength	250 MPa
Tensile ultimate strength	460 MPa

It should be noted that the interaction of double parallel cracks was examined under different types of loading, tension, bending, and mixed-mode loading. In the case of mixed-mode loading, tension, bending, and torsion are combined and applied to the cracked structure. Generally, based on the literature, the vast majority employed remote constant loading in their research. Therefore, all the above-mentioned loads were applied remotely to the cylinder by using a remote point, meanwhile, it is frequently applied. Moreover, the remote point was linked to one end of the cylinder, where the load was applied through it, while the other end was fixed with zero displacements in all degrees of freedom.

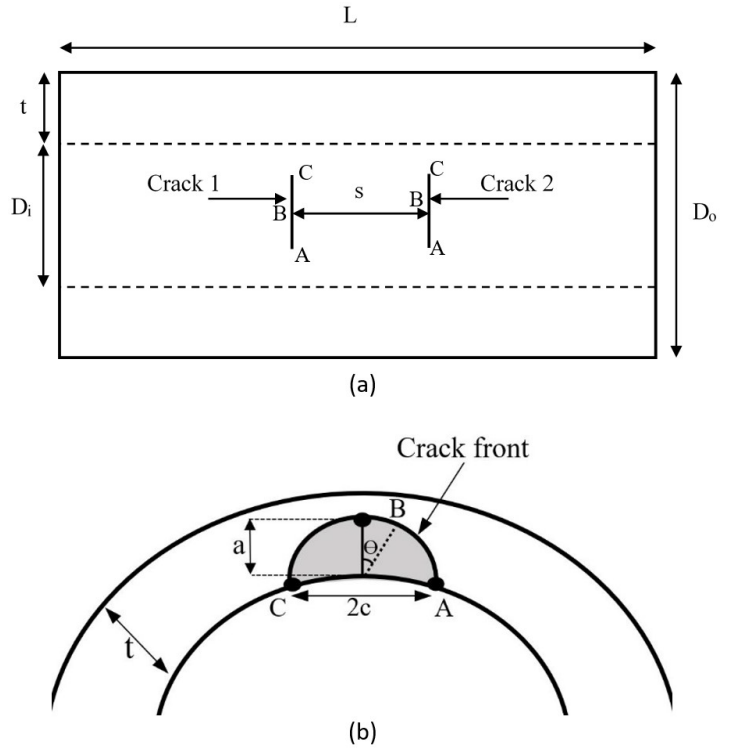

Figure 1. *Parallel cracks configuration (a) topmost view (b) points on the crack front*

3 SOLUTION METHOD

In this section, the solution method is described in four phases. The first phase contains the description of the finite element model in terms of mesh and geometry as well as loading and boundary conditions. In the second phase, the method utilized to determine SIFs was introduced. The obtained SIFs in the second phase were utilized in the third phase to determine the interaction factor. Finally, the correlation techniques that have been employed to characterize the relationship between SIFs of single and double cracks are introduced in the fourth phase.

3.1 Finite element model

The finite element software Ansys has been utilized to model and analyze the cracked thick and thin cylinders using dimensions stated in Table 1. Notably, the cracks initially start with an irregular shape, but this shape evolves and converts to a semi-elliptical geometry within a few recurrent loads (Lin and Smith 1998). Therefore, the cracks are modelled with a semi-elliptical crack shape. Since two types of cylinders were used, thus, for each cylinder type different crack geometries were used as shown in Table 3.

From Figure 2, it is obvious that dual types of mesh were applied for the present analysis, where an identical fine mesh is employed in the regions surrounding the crack and a coarse mesh is used elsewhere. For the coarse mesh, a tetrahedral mesh was used, with a quadratic order of elements, while for the fine mesh, in the region of the crack, a mesh with hexahedral elements was used. Both types of mesh were recommended by (ANSYS Mechanical APDL Fracture Analysis Guide, 2019).

Table 3. Crack geometry

		Thick cylinder		Thin cylinder	
a/c	***a/t***	***a, mm***	***c, mm***	***a, mm***	***c, mm***
	0.2	5	12.5	2	5
0.4	0.5	12.5	31.25	5	12.5
	0.8	20	50	8	20
	0.2	5	8.3333	2	3.333
0.6	0.5	12.5	20.833	5	8.333
	0.8	20	33.333	8	13.333
	0.2	5	6.25	2	2.5
0.8	0.5	12.5	15.625	5	6.25
	0.8	20	25	8	10
	0.2	5	5	2	2
1.0	0.5	12.5	12.5	5	5
	0.8	20	20	8	8
	0.2	5	4.1666	2	1.666
1.2	0.5	12.5	10.416	5	4.166
	0.8	20	16.666	8	6.666

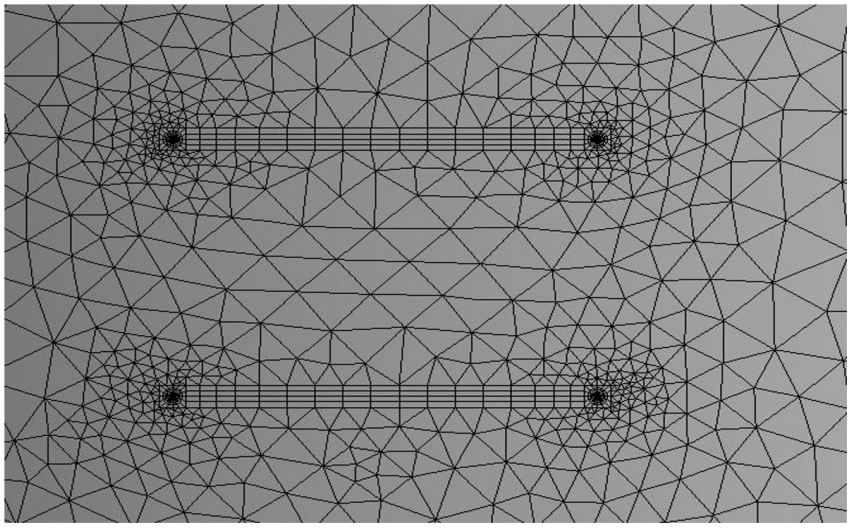

Figure 2. *Close view of the parallel crack configuration*

For loading, three types of loading were applied to examine the double parallel cracks interaction. Furthermore, tension as well as bending are applied separately, and mixed-model loading consists of a combination of tension, bending, and torsion. Generally, based on the literature, the vast majority employed remote loading in their research, therefore this study employed the same.

3.2 SIFs calculations

As it is known, it has been found that Finite Element Methods (FEM) is an efficient tool in solving multiple cracks interaction problems due to the complexity of the geometry (Diamantoudis and Labeas 2005). Therefore, Ansys, the FE software, has been utilized in the present study to model and analyze the double cracks problem. In Ansys, there are two methods to determine the SIFs (Al Emran Ismail et al. 2018):

1. Displacement Extrapolation Method (DEM)
2. Interaction Integral Method (IIM)

In DEM, the SIFs are determined by describing the displacement between two nodes placed along the crack faces surrounding the crack tip. While in the IIM for the SIFs computation uses area integration for 2-D problems and volume integration for 3-D problems. However, the IIM compared to DEM presents better precision, less mesh obligation, and is easy to use. Therefore, in the present study, IIM was selected to calculate the SIFs.

Ansys provides the capability to generate unlimited numbers of contours around the crack tips which are numbered in a radial fashion. The SIFs at each contour are determined; where six contours were created around the crack tips in the entire examination, as illustrated in Figure 3. Due to the contraction of the material near the crack tips (Rice 1968), the results of the nearest contour to the crack tip were neglected. Also, it was found that there is no significant difference between the fifth and sixth contours compared to that found between the first and the sixth; however, the results of the sixth contour were selected.

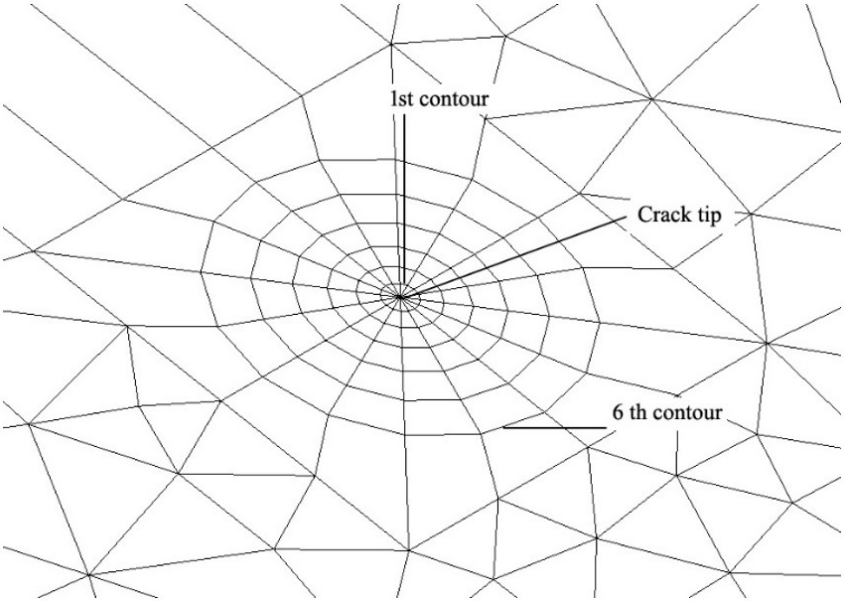

Figure 3. *Contours alignment around the crack tip*

After collecting the SIFs, normalization of the SIFs is required. By the use of normalization, it is easy to compare two different cracked structures having similar crack formations. Therefore, the normalization of SIFs facilitates the comparison process and ensures the generality of the results. Also, normalization eliminates the geometry effects. It should be noted that based on the literature, a separate equation is utilized for the normalization depending on the type and mode of loading. For tension and bending loading, the following formulas are utilized to normalize mode I SIFs (Raju and Newman 1986):

$$F_t = \frac{K_{cal,t}}{\sigma_t \sqrt{\pi a/Q}} \tag{1}$$

$$F_{Ben} = \frac{K_{cal,b}}{\sigma_b \sqrt{\pi a/Q}} \tag{2}$$

Where F_t is the normalized SIFs under remote tension loading, $K_{cal,\ t}$ is the calculated SIFs under tension (the extracted value from the 6th contour), σ_t is the axial stress. Similarly, F_{Ben} is the normalized mode I SIFs under remote bending loading, $K_{cal,\ b}$ is the calculated SIFs under bending (extracted from Ansys), σ_b is the maximum bending stress. On the other hand, a is the crack depth, and Q is the shape factor defined in the following (Raju and Newman 1982):

$$\mathrm{Q} = 1 + 1.464(^{\mathrm{a}}/_{\mathrm{c}})^{1.65} \text{ for a/c} \leq 1 \tag{3}$$

$$Q = 1 + 1.464(^{c}/_{a})^{1.65} \text{ for a/c} > 1 \tag{4}$$

Furthermore, for the mixed-mode loading case, where the applied load is tension, bending and torsion, applied simultaneously to the examined structure, SIFs from all three modes were determined as a result of the aforementioned method of loading, and each mode was then normalized independently. Lastly, normalized SIFs are given by equivalent SIFs, F_{EQV}, as a result of the combined load, that is (A. E. Ismail et al. 2012):

$$F_{EQV} = \sqrt{(F_I)^2 + (\lambda F_{II})^2 + \left(\frac{\lambda F_{III}}{1-\nu}\right)^2} \tag{5}$$

Correspondingly, F_I, $F_{II,}$ and F_{III} demonstrate normalized SIFs related to mode I, II, and III under mixed-mode loading, besides λ is a proportion given by:

$$\lambda = \frac{\tau}{\sigma_b} \tag{6}$$

Where τ is the shear stress. Finally, the normalized SIFs distribution is presented along the crack front as a function of the normalized crack front position. The normalized crack front position is a non-dimensional coordinate that may be used to specify any place on the crack front. The utilized formula to normalize the position is 2Θ/π, where Θ, is the parametric angle of the crack. Therefore, when 2Θ/π = (-1or 1), this value represents surface points A and C Figure 1(b), while 2Θ/π =0, denoting the deepest point on the crack front, point B Figure 1(b).

3.3 Interaction factor

As it is aforementioned, the normalized SIFs were calculated for each mode and type of loading; then the interaction factor must be determined. The interaction factor Ψ is defined as the ratio of two crack SIFs to that of a single crack; therefore, the following expression is used to determine the interaction factor (Omar Mohammed Fakhri 2021) :

$$\Psi = \frac{F_{two\ cracks}}{F_{single\ crack}} \tag{7}$$

Where $F_{\text{two cracks}}$ represents the normalized SIFs for the case of two cracks for any mode and type of loading, and $F_{\text{single crack}}$ is the normalized SIFs for the case of single crack. Moreover, the Ψ for tension loading, for instance, is the ratio of the normalized SIFs for the case of two cracks with respect to normalized SIFs for the single crack case in tension loading also. This procedure applies to the remaining types and modes of loadings. It should be noted that $F_{\text{two cracks}}$ obtained in this study are compared to $F_{\text{single crack}}$ obtained by the same authors in (O. M. Fakhri et al. 2019), (Al-moayed et al. 2020), and (Al-Moayed et al. 2019) for single circumferential cracked thick and thin cylinders under different types of loading.

Alternatively, the crack interaction effect on the SIFs could be classified into three categories. The initial is the amplification or enhancement influence, which indicates that the normalized SIFs for two cracks were proved to be greater than those of a single crack owing to the crack interaction. The next type is the shielding impact, the normalized SIFs for the two cracks case were found to be less than those of a single crack. The last category represents the situation of no interaction among the cracks, hence each crack could be treated as a standalone crack. Built on the aforesaid three categories, it is essential to organize the judgment rules. Thus, Ψ impact classification is described by the subsequent formulas:

$$\Psi > 1 + \Psi_c \tag{8a}$$

$$\Psi < 1 - \Psi_c \tag{8b}$$

consequently

$$1 - \Psi_c > \Psi > 1 + \Psi_c \tag{9}$$

Where Ψ_c is the critical or the tolerance value, which was set to 5%. Based on Equation (8), it should be no interaction when Ψ =1, therefore, Equation (8a) represents the amplification effect, while the shielding effect is represented by Equation (8b). Moreover, the values that lie in between the two limits are treated as isolated cracks. It should be noted that the same tolerance range or the critical value Ψ_c has been considered in (Anis et al. 2020).

3.4 Correlation techniques

The correlation is a statistical procedure that can validate whether and in what manner powerfully pairs of variables are associated. Correlation analysis is a statistical approach applied to assess the strength of the connection between two quantitative variables. A high correlation indicates that multiple variables share a strong link with each other, whereas a low correlation indicates that the variables are barely associated. In simple terms, it is a way of evaluating the strength of the association using data that is readily available (Franzese and Iuliano 2019). Because one of the primary goals of this research is to describe the link between the SIFs of single and multiple cracks, it is critical to use correlation approaches to accomplish this goal.

The commonly utilized method for correlation purposes is Regression. Regression analysis is a means of identifying which factors may have an impact statistically. The importance of regression analysis in any subject stems from its ability to discover which elements are most important, which may be ignored, as well as how all of them affect one another. Predicting using the regression approach entails investigating the correlations between data items (Gallo 2015). Thus, the regression method has been chosen to implement the correlation between the SIFs values for single and double cracks.

Moreover, in the current study linear regression has been employed to obtain the relationship between the SIFs for single and double cracks, where the SIFs for single crack are utilized to estimate the SIFs for double surface cracks in the case of parallel cracks. Also, the calculated SIFs for single and double cracks, which were determined by Ansys assumed

to be the X and Y, correspondingly. In addition, due to the enormous calculation processes and in order to reduce the calculation time, MATLAB software has been used to conduct the regression. The required procedure which is utilized in MATLAB to perform the regression is explained in Table 4.

Table 4. Pseudocode of linear regression

```
Begin
Input
    X[]; // data for SIFs for single crack
    Y[];// data for SIFs for double cracks
  For (i=0, i=x-1, i++)
    p1=polyfit(x,y,1);
    yfit=p1(1)*x+p1(2);
    yresid=y-yfit;
    SSresid=sum(yresid.^2);
    SStotal= (length(y)-1) * var(y)
    rsq=1-SSresid/SStotal;
    plot(x,y)
  End
End
```

4 RESULTS

The results of the current study will be introduced in the following sequence, validation of the model, then the distribution of SIFs for single and double cracks. Next, the interaction factor is introduced for the examined cases, and finally, the empirical mathematical model is introduced along with the validation of the model.

4.1 Model validation

One of the primary tasks in the present study is to validate the proposed thick and thin cylinder models. Validation permits to carry out the analysis utilizing the proposed model.

Table 5. Validation of single circumferential crack in a thick cylinder

Reference	Deepest point			Surface point		
	a/t			a/t		
	a/c =0.6					
	0.2	0.5	0.8	0.2	0.5	0.8
Reference (Raju and Newman 1986)	1.101	1.178	1.285	0.933	1.071	1.285
Present	1.074	1.160	1.243	0.911	1.027	1.243
Error %	2.45	1.52	3.26	2.35	4.10	3.26
			a/c =0.8			
Reference (Raju and Newman 1986)	1.058	1.103	1.157	1.053	1.156	1.333
Present	1.048	1.114	1.161	1.034	1.161	1.366
Error %	0.94	0.99	0.34	1.80	0.43	2.47
			a/c= 1.0			
Reference (Raju and Newman 1986)	1.019	1.046	1.072	1.154	1.234	1.381
Present	1.036	1.079	1.110	1.138	1.259	1.412
Error %	1.66	3.15	3.54	1.38	2.02	2.24

Due to the absence of a similar model to the present examined model, thus, each of the thick and thin cylinders with a single circumferential crack was used for validation purposes. Furthermore, the normalized SIFs of the cracked configurations of the proposed models were compared to those of (Raju and Newman 1986) under tension loading. It has been assumed that the maximum difference between the obtained SIFs and those obtained by (Raju and Newman 1986) should not exceed 5%. As depicted in Table 5, SIFs for three values of *a/c* have been compared, where each value of *a/c* was examined for three values of *a/t* for a single circumferential crack in a thick cylinder. The maximum error

found between these results was equal to 4.10%. Based on the comparison, the thick cylinder proposed model seems to be in good agreement and eligible for further analysis.

Table 6. Validation of single circumferential crack in thin cylinder

Reference	Deepest point			Surface point		
	a/t			a/t		
	a/c =0.6					
	0.2	0.5	0.8	0.2	0.5	0.8
Reference (Raju and Newman 1986)	1.097	1.167	1.247	0.930	1.070	1.290
Present	1.072	1.155	1.201	0.907	1.031	1.235
Error %	2.270	1.020	3.680	2.470	3.640	4.260
			a/c =0.8			
Reference (Raju and Newman 1986)	1.057	1.101	1.144	1.051	1.156	1.335
Present	1.043	1.103	1.102	1.018	1.137	1.318
Error %	1.320	0.180	3.670	3.130	1.640	1.270
			a/c= 1.0			
Reference (Raju and Newman 1986)	1.020	1.049	1.074	1.152	1.233	1.380
Present	1.028	1.069	1.051	1.119	1.221	1.385
Error %	0.780	1.900	2.140	2.860	0.970	0.360

Alternatively, Table 6 displays the comparison of the single circumferential crack in a thin cylinder of the present model with respect to that of (Raju and Newman 1986) in terms of the normalized SIFs. As it is evident, all the error values fall within an acceptable limit, and the maximum difference was found to be equal to 4.26%. Therefore, the proposed thin cylinder model compared to the available model in the literature is found to be with a satisfactory agreement and this model is qualified to be exploited for the double crack problem. It should be noted that many factors are affecting the discrepancy between the obtained results using the proposed model and those found in the literature. For example, since this study utilizes FEM, mesh in general considered one of the most affecting factors, in terms of method, size, and element type. Also, some of the utilized mathematical methods such as rounding may lead to the difference between the two tested values. However, since the value of the error remains below 5% which is the commonly used value, the proposed model is considered valid and eligible to use.

4.2 SIFs distribution

The double parallel cracks configuration consists of two similar parallel cracks separated by an axial distance *s*, which has been used in the normalized form, *s/L*, where *L* is the overall span of the cylinder. The two parallel cracks were placed either on the outside or inside surface of the thick and thin cylinders. However, under examined types of loading, the results showed no significant difference between SIFs for external and internal cracks, thus results for external cracks only are presented. Moreover, SIFs distribution along the crack front is described in terms of the position of the crack front, where SIFs for single and double parallel cracks are presented as a function of the normalized separation distance *s/L*.

It should be remarked that the normalized SIFs of the single crack are identified as F_SINGLE, while the normalized SIFs in the case of two cracks, F_2, are labeled according to the normalized separation distance between cracks *s/L*. Likewise, F_2 – s/L=0.004 represents the normalized SIFs for the case of two cracks when the separation distance ratio between the two cracks *s/L* is equal to 0.004, and so on for the other remaining distributions. Also, the distribution of the normalized SIFs for the case of parallel cracks configuration was found to be similar at both cracks; therefore, the distribution of crack-1 is presented. Similarly, due to the same trend shown by the SIFs distribution for the considered *a/c* range; thus, results for only *a/c*=0.4 and 1.2 were introduced under each of tension, bending, and mixed-mode loading in the subsequent figures. Lastly, in terms of SIFs trend along the crack front, both thick and thin cylinders displayed similar behavior. Consequently, only SIFs distribution on thick cylinder is introduced in this study.

Figure 4 illustrates the distribution of the normalized SIFs for exterior double parallel cracks subjected to tension loading F_{t-EXT}, where *a/c* =0.4 for *a/t*= 0.2, 0.5, and 0.8, respectively. It is obvious that F_{t-EXT} is scattered equally along the crack front despite the existence of crack interaction. Also, *a/t* has a noticeable influence on the F_{t-EXT} trend, where the highest F_{t-EXT} is attained for the maximum *a/t* value and vice versa. It can be noticed that F_{t-EXT} distribution followed an exactly similar tendency to that of a single crack for all the examined *s/L* ratios. It can be inferred from graphs that as the distance between the cracks increases (*s/L* ratio increases) F_{t-EXT} approaches to the F_SINGLE value. This means the

crack interaction has a high influence when the cracks are placed close to each other, while as the separation distance between the cracks increases, each crack is found to be isolated from the other. This is what has been interpreted by the similar value of single crack to that of double cracks, especially for small *a/t* at *s/L*=0.032, where no interaction impact. Therefore, the minimum SIFs attained at F_2 – *s/L*=0.004, and the maximum SIFs attained at F_2 – *s/L*=0.032, where both values are considered minimum and maximum with respect to the normalized SIFs for the single crack case. In addition, for the same examined *a/c*, the effect of *s/L* was found to be more pronounced for *a/t* ≤ 0.5.

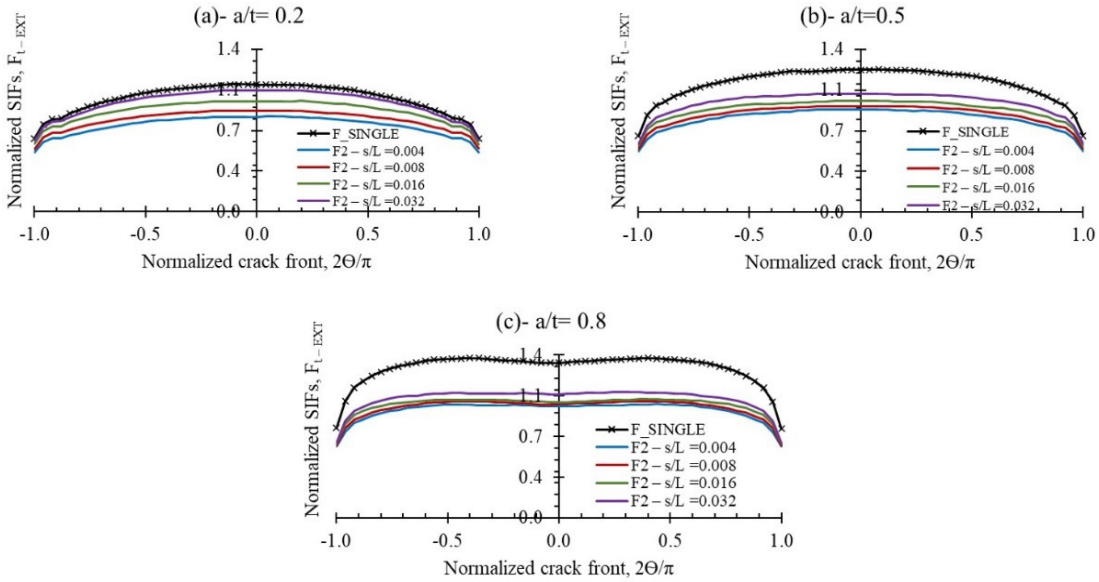

Figure 4. SIFs for external double parallel cracks in a thick cylinder under tension for a/c=0.4

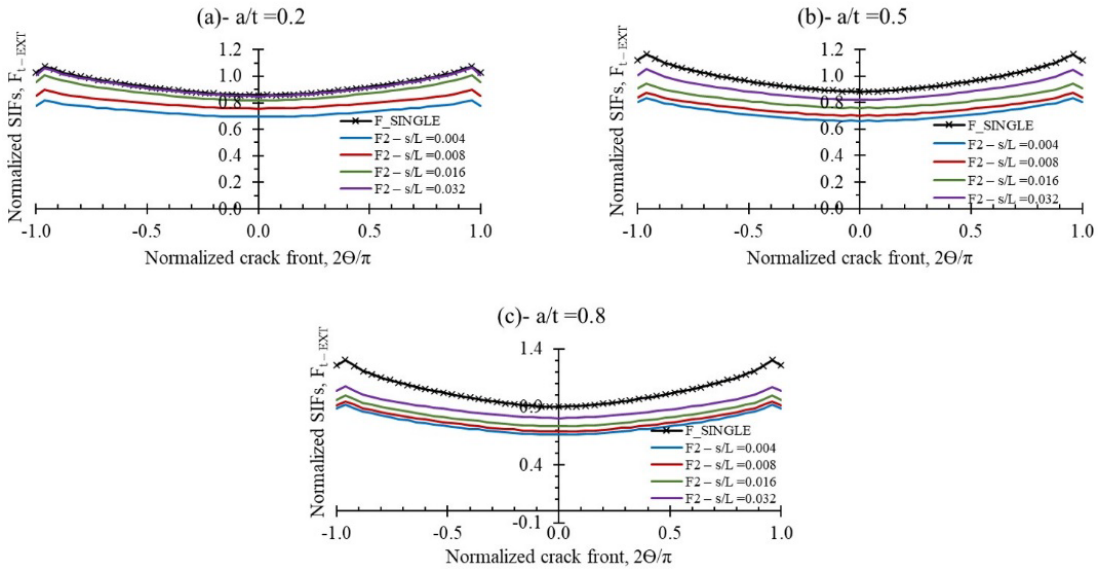

Figure 5. SIFs for external double parallel cracks in a thick cylinder under tension for a/c=1.2

Figure 5 explains the trend F_{t-EXT} as a function of the normalized crack front position when *a/c*=1.2 for *a/t*= 0.2, 0.5, and 0.8. It is found that F_{t-EXT} for *a/*c=1.2 followed the same behavior as that displayed when *a/c*=0.4 in terms of *a/t* as well as *s/L* influence on the SIFs distribution. Except, the presence of the transition effect, which is a well-known phenomenon. It has been shown that for each *a/t* there is a specific *a/c* in which the position of the maximum SIFs shifts from the deepest point on the crack front (B) to the surface points (A) and (C) as stated by (Carpinteri 1993). Since F_{t-EXT} for two double parallel cracks followed the same manner exhibited by a single crack, thus, the influence of *a/c* and *a/t* on SIFs with respect to A and C could be displayed using SIFs for a single crack.

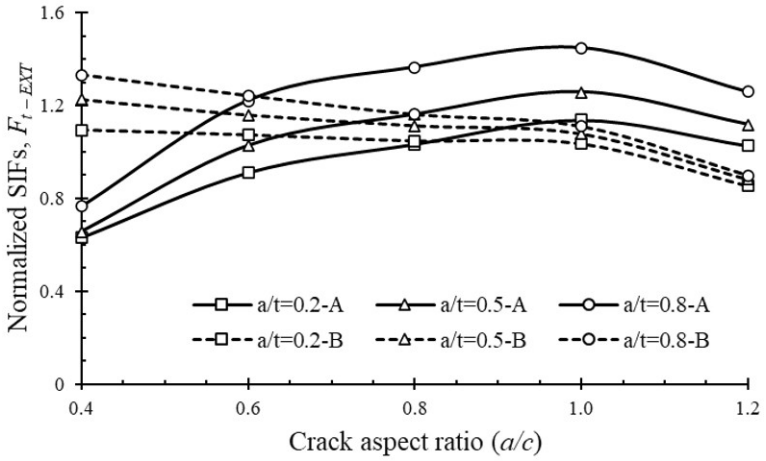

Figure 6. Effect of crack geometry on the surface and deep point on the crack front

Figure 6 clarifies the behaviour of F_{t-EXT} as a function of a/c and a/t at both surface and deepest points on the crack front A and B, respectively. It is evident that a/t has a similar effect on F_{t-EXT} at A and B, where F_{t-EXT} increases with the increase of a/t. On the other hand, the increase of a/c has two different impacts on each of A and B. Moreover, the increase in a/c at B was found to be accompanied by a decrease in F_{t-EXT} along with an insignificant effect for a/t when a/c=1.2. Besides, at A the increase of crack aspect ratio for $0.4 \le a/c \le 1.0$ produces an increment in F_{t-EXT}, while F_{t-EXT} decreases for a/c>1.0.

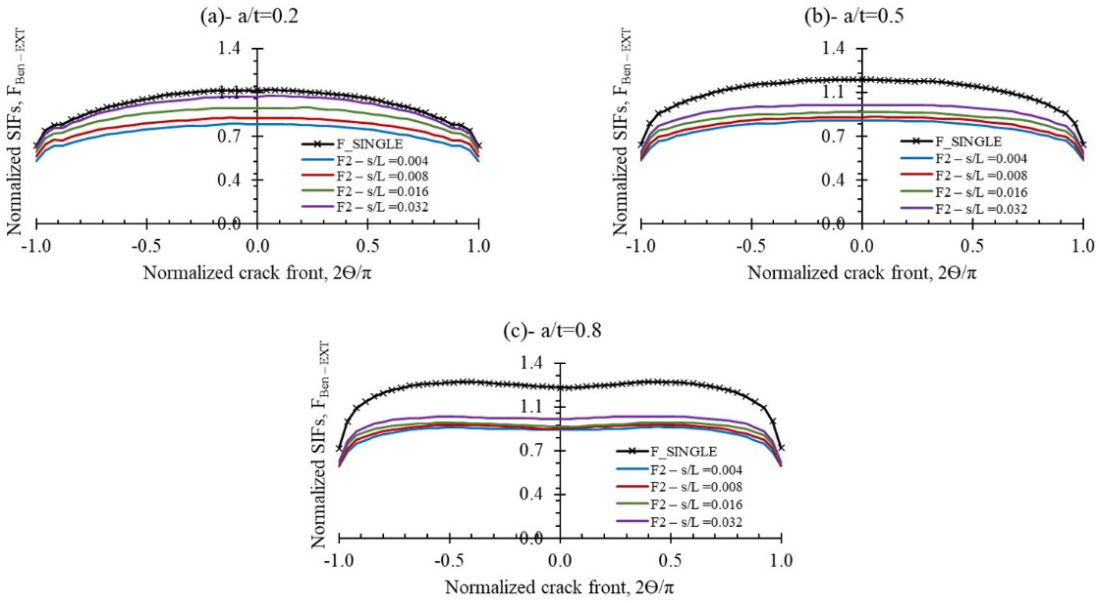

Figure 7. SIFs for external double parallel cracks in a thick cylinder under bending for a/c=0.4

The distribution of the normalized SIFs for parallel exterior cracks exposed to bending loading, $F_{Ben-EXT}$ is shown in Figures 7 and 8 when a/c= 0.4 and 0.8, respectively. Generally, $F_{Ben-EXT}$ trend was found to be similar to that of F_{t-EXT} with a slightly lower magnitude. Also, the change in a/t ratio produces the same effect which was shown by the same crack configuration underneath tension loading, where cracks with a high value of a/t showed higher $F_{Ben-EXT}$ compared to cracks with less a/t.

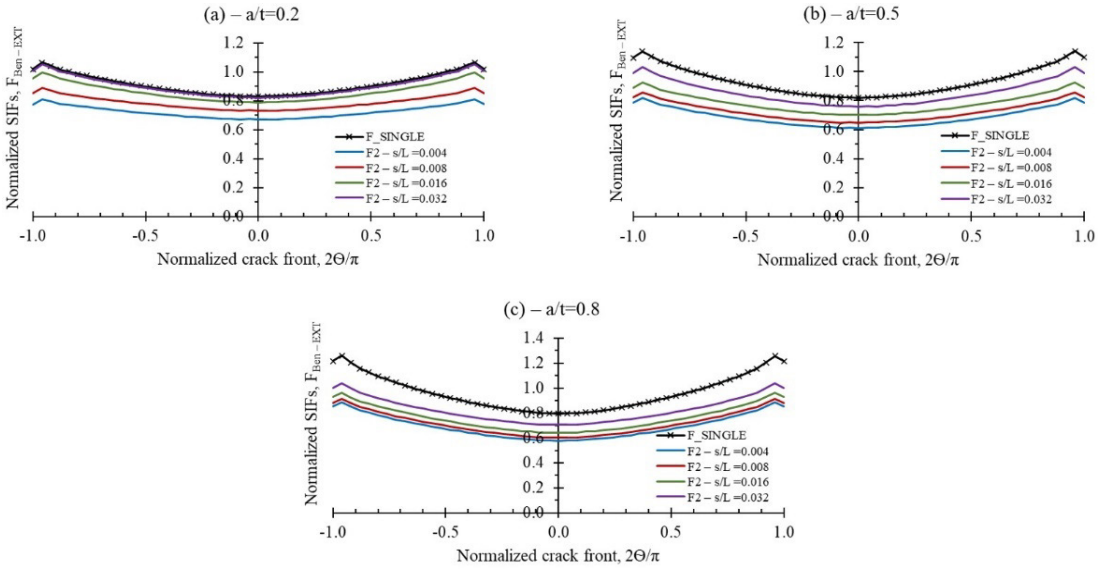

Figure 8. SIFs for external double parallel cracks in a thick cylinder under bending for a/c=1.2

Also, the distribution of $F_{Ben-EXT}$ on A and B exhibited the same trend shown by F_{t-EXT} in terms of *a/c* and *a/t*. It should be noted that the value of $F_{Ben-EXT}$ was found to be less than that of F_{t-EXT} for the same examined crack configurations.

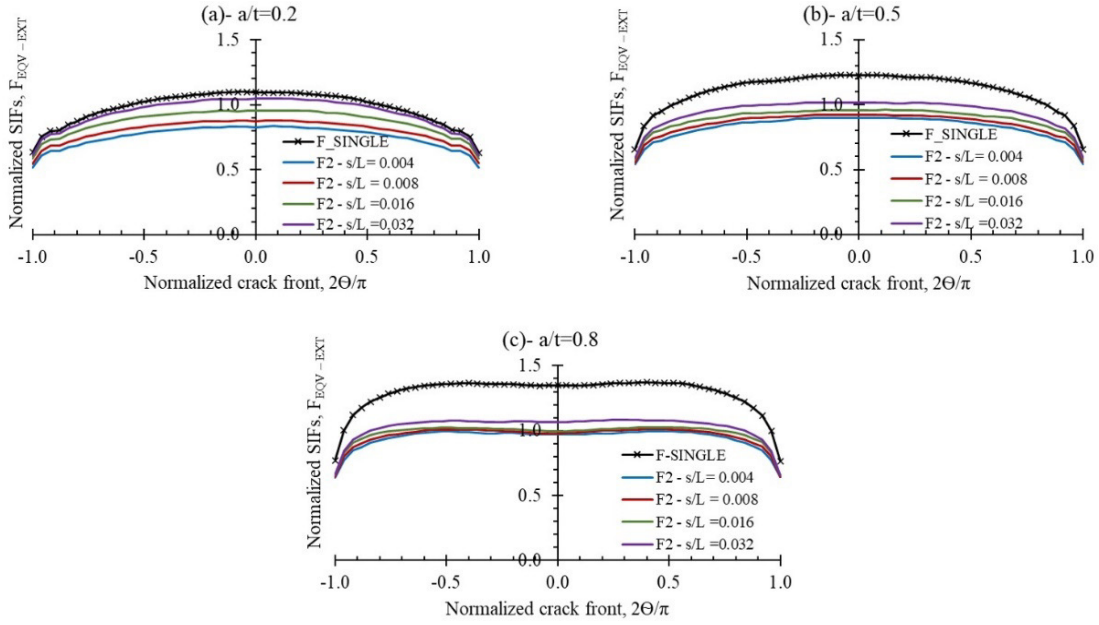

Figure 9. SIFs for external double parallel cracks in a thick cylinder under mixed-mode for a/c=0.4

Figures 9 and 10 demonstrate the tendency of the normalized SIFs for single and double parallel cracks beneath mixed-mode loading $F_{EQV-EXT}$, when *a/c*=0.4 and 1.2 for *a/t*=0.2, 0.5, and 0.8. It can be inferred from the graphs that for the same *a/c*, *a/t* has a direct proportion with $F_{EQV-EXT}$, where the rise in *a/t* produced a remarkable increment in $F_{EQV-EXT}$. Also, the $F_{EQV-EXT}$ distribution along the crack front followed an identical manner to that of tension and bending loading, where for low *a/c* the trend was observed to be following a convex curve shape, while for high *a/c* it was following a concave curve shape. This includes the predefined phenomenon, the transition effect, which has been explained earlier.

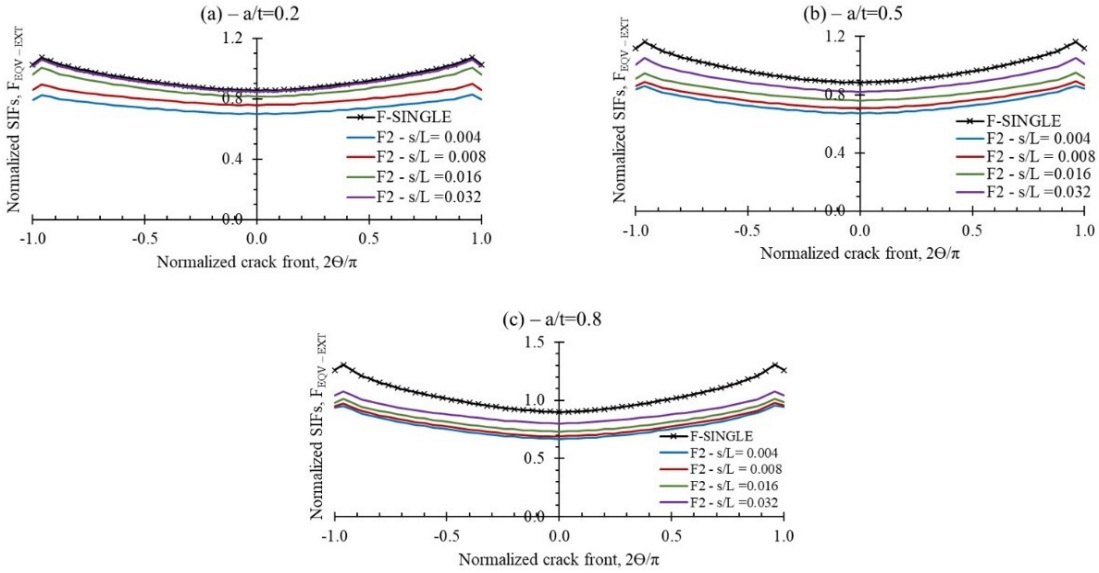

Figure 10. SIFs for external double parallel cracks in a thick cylinder under mixed-mode for a/c=1.2

Generally, in terms of interaction influence under the abovementioned types of loading, all examined cases exhibited an obvious shielding effect. This could be interpreted by the highest value of F_SINGLE compared to the others of double parallel cracks. Furthermore, as the cracks are positioned close to each other, the greater the interaction impact, the stress field is relaxed; thus, leading to a high reduction in SIFs. Also, the crack interaction criteria in API 579-1 standard (API 2016) produced more conservative results. Moreover, despite considering the separating distance greater than what has been stated in the standard, the normalized SIFs for double cracks (especially for cracks with $a/t \geq 0.5$) did not approach F_SINGLE. This indicates that the crack interaction still affects the SIFs on each crack.

It should be noted that this shielding effect was found to be in an inverse relationship with the horizontal separation distance, as the separation distance increases the interaction impact is reduced. This interaction influence for double parallel cracks was found to be similar to that of parallel cracks found in plates (Han, Qian, and Li 2020) and in solid cylinders (Awang et al. 2017), where both studies explored the interaction influence of parallel cracks. However, in order to quantify this rate of interaction between the cracks, the interaction factor (Ψ) is determined for this purpose in the next section.

4.3 Interaction factor

The interaction factor Ψ which is defined in Equation 9 was obtained for double parallel cracks in order to quantify the interaction value under the examined types of loading. Also, Ψ introduced for two points only on the crack front they are A and B Figure 1(b) because SIFs at A and C are the same. In addition, Ψ presented in a tabulated form, where both thick and thin cylinders are considered. Besides, A_0 and B_0 are denoted to the surface and deep points when s/L=0.004 (the minimum examined distance), while A_1 and B_1 represent the same points when s/L=0.032 (the maximum examined distance). In other words, the interaction factor for double cracks presented for thick and thin cracked cylinders at A and B for the minimum and maximum separation distances, s/L=0.004 and 0.032, respectively.

Table 7 shows Ψ in terms of the examined crack geometry a/c, and a/t at two points on the crack front for double parallel cracks placed on thick and thin cylinders under tension loading. As discussed for the normalized SIFs orientation along the crack front, the presence of double parallel cracks produced shielding influence on the SIFs. Therefore, based on Equation 9, Ψ should be less than unity.

Obviously, the maximum shielding influence is observed when the cracks are located close to each other (A_0 and B_0), while the minimum impact is noticed when the cracks are positioned utilizing the farthest examined distance (A_1 and B_1). Also, it was clear that the interaction influence for the cracks located on thick cylinder was found to be higher than those of similar cracks located on thin cylinder. Moreover, the reduction amount in SIFs due to interaction in cracked thick cylinder was greater than that of thin cylinder, especially for cracks with $a/t \leq 0.5$. For example, when a/c=1.0, for a/t=0.2, the reduction rate at A_0 is equal to 24.5% for a thick cylinder, while for the same crack on a thin cylinder, the reduction is equal to 16%.

Similarly, at B_0 the SIFs reduction is equal to 21.2% and 12.1% for thick and thin cylinders, respectively. However, for a/t=0.8, the high discrepancy between the reduction amount on each thick and thin cylinders becomes insignificant, since the difference does not exceed 5%. The aforementioned example is applicable to all examined a/c ratios. On the other hand, Ψ at each of A and B for the maximum examined separation distance s/L (A_1 and B_1), proved that double

parallel cracks with *a/t*=0.2 located on thick and thin cylinders are isolated from each other. This means each crack is considered free from the neighboring crack influence.

Table 7. Interaction factors under tension loading

Thick cylinder				Thin cylinder		
			a/c=0.4			
Point	**0.2**	**0.5**	**0.8**	**a/t**	**0.2**	**0.5**	**0.8**
A_0	0.806	0.800	0.808		0.880	0.836	0.825
B_0	0.745	0.721	0.723		0.811	0.755	0.705
A_1	0.967	0.893	0.843		0.994	0.935	0.853
B_1	0.954	0.829	0.797		0.994	0.935	0.865
			a/c=0.6			
A_0	0.771	0.741	0.738		0.853	0.786	0.767
B_0	0.755	0.724	0.712		0.832	0.760	0.758
A_1	0.973	0.875	0.808		0.994	0.949	0.876
B_1	0.965	0.857	0.813		0.995	0.957	0.912
			a/c=0.8			
A_0	0.758	0.721	0.708		0.821	0.771	0.749
B_0	0.773	0.727	0.719		0.851	0.775	0.746
A_1	0.980	0.877	0.804		1.000	0.966	0.902
B_1	0.982	0.885	0.840		1.004	0.974	0.940
			a/c=1.0			
A_0	0.755	0.717	0.701		0.840	0.769	0.743
B_0	0.788	0.738	0.724		0.879	0.793	0.760
A_1	0.982	0.888	0.810		1.002	0.977	0.926
B_1	0.984	0.911	0.870		1.006	0.984	0.970
			a/c=1.2			
A_0	0.756	0.717	0.701		0.854	0.770	0.744
B_0	0.811	0.748	0.732		0.902	0.812	0.776
A_1	0.983	0.901	0.822		1.002	0.983	0.941
B_1	0.991	0.929	0.892		1.004	0.989	0.974

Nevertheless, for $a/t \geq 0.5$, Ψ in the thick cylinder does not approach the isolation value (0.95 – 1.0) for all examined *a/c*, while the same behaviour was noticed on the thin cylinder when *a/t*=0.8, except for *a/t*=0.5 where the cracks isolated. Consequently, it can be inferred that the available interaction criteria alignment rules for acceptable interaction ranges could produce unrealistic results. Moreover, based on the interaction criteria all Ψ values for A_1 and B_1 should lie between 0.95 to 1.0, this was appropriate for *a/*t =0.2, but for $a/t \geq 0.5$, Ψ does not approach this value.

However, the results implied that the current interaction criteria have to be modified, which is the same as that was recommended in (G. Coêlho, Silva, and Santos 2022; G. de C. Coêlho et al. 2019). Utilizing crack geometry such as crack length and depth along with the thickness of the examined body to formulate new or modify the current interaction criteria could provide enhancement and eliminate underestimation.

Tables 8 and 9 introduce the interaction factor for double parallel cracks located on thick and thin cylinders under bending and mixed-mode loading, respectively. The behaviour of Ψ in terms of crack geometry as well as the horizontal separation distance found to be similar to that shown under tension loading. Since in all examined loading the dominant type of failure was mode I, thus no significant difference in Ψ values. In addition, it should be noted that the maximum interaction rate occurs at a position depending on the position of the maximum SIFs on the crack front, if maximum SIFs lie on the deepest point, the maximum interaction rate is attained at the deepest point, and vice versa for surface points.

However, based on the interaction level with respect to cylinder type, the results depicted that, cracks in thick cylinders (external and internal) showed a high rate of interaction compared to those of thin cylinder. Since the interaction impact was demonstrated by shielding influence only, thus, a thick cylinder has high resistance against crack propagation due to the difference in the wall thickness.

Table 8. Interaction factors under bending loading

Thick cylinder				Thin cylinder		
			a/c=0.4			
Point	0.2	0.5	0.8	a/t	0.2	0.5	0.8
A_0	0.804	0.800	0.800		0.880	0.836	0.820
B_0	0.743	0.719	0.720		0.810	0.753	0.717
A_1	0.965	0.895	0.834		0.994	0.935	0.861
B_1	0.954	0.825	0.791		0.994	0.934	0.862
			a/c=0.6			
A_0	0.767	0.742	0.737		0.850	0.785	0.766
B_0	0.754	0.721	0.708		0.831	0.758	0.756
A_1	0.971	0.876	0.808		0.994	0.948	0.876
B_1	0.965	0.853	0.806		0.995	0.956	0.910
			a/c=0.8			
A_0	0.758	0.721	0.708		0.840	0.772	0.749
B_0	0.771	0.724	0.716		0.850	0.773	0.743
A_1	0.979	0.878	0.805		1.000	0.967	0.903
B_1	0.982	0.882	0.833		1.004	0.974	0.939
			a/c=1.0			
A_0	0.758	0.717	0.702		0.850	0.770	0.742
B_0	0.786	0.735	0.720		0.878	0.791	0.757
A_1	0.983	0.889	0.813		1.002	0.977	0.926
B_1	0.984	0.908	0.863		1.006	0.984	0.969
			a/c=1.2			
A_0	0.761	0.717	0.702		0.860	0.772	0.743
B_0	0.808	0.746	0.728		0.901	0.811	0.773
A_1	0.987	0.902	0.825		1.002	0.983	0.941
B_1	0.989	0.926	0.886		1.004	0.988	0.974

Table 9. Interaction factors under mixed-mode loading

Thick cylinder				Thin cylinder		
			a/c=0.4			
Point	0.2	0.5	0.8	a/t	0.2	0.5	0.8
A_0	0.821	0.826	0.838		0.886	0.857	0.845
B_0	0.755	0.735	0.721		0.816	0.763	0.752
A_1	0.968	0.899	0.853		0.996	0.936	0.863
B_1	0.954	0.830	0.789		0.993	0.935	0.864
			a/c=0.6			
A_0	0.788	0.774	0.779		0.859	0.814	0.814
B_0	0.765	0.737	0.720		0.836	0.767	0.767
A_1	0.973	0.879	0.818		0.995	0.948	0.883
B_1	0.966	0.856	0.814		0.995	0.956	0.912
			a/c=0.8			
A_0	0.775	0.756	0.754		0.836	0.803	0.804
B_0	0.783	0.741	0.732		0.853	0.782	0.752
A_1	0.981	0.880	0.812		1.001	0.968	0.907
B_1	0.982	0.886	0.845		1.004	0.974	0.941
			a/c=1.0			
A_0	0.771	0.751	0.749		0.854	0.803	0.801
B_0	0.797	0.752	0.731		0.881	0.800	0.766
A_1	0.982	0.889	0.817		1.016	0.981	0.925
B_1	0.985	0.912	0.867		1.005	0.984	0.970
			a/c=1.2			
A_0	0.774	0.751	0.748		0.863	0.802	0.802
B_0	0.817	0.761	0.742		0.903	0.818	0.783
A_1	0.987	0.902	0.826		1.011	0.985	0.941
B_1	0.989	0.928	0.891		1.004	0.989	0.974

4.4 Correlation

The correlation between single and double parallel cracks has been demonstrated by an empirical mathematical model applicable to dual parallel cracks exposed to tension, bending, and mixed-mode loading. The regression has been performed to obtain the relationship between the obtained SIFs for single and parallel double cracks. Moreover, it has been found that by using SIFs for a single crack, it is possible to predict SIFs for two parallel cracks according to the separation distance between the cracks. In addition, the proposed empirical model has been designed to include a wide range of crack geometry, such as crack aspect ratio and relative crack depth. Besides, the ability to predict SIFs for double cracks at any point on the crack front since it exhibited a high rate of accuracy when validated using performance evaluation metrics. The empirical mathematical model is presented in Equations 10 to 17, where Equations 10 to 13 are dedicated to thick cylinders, while Equations 13 to 17 are for thin cylinders, each equation dedicated to a specified separation distance *s*. The accuracy and ability of the proposed model along with the specified separation distance for each equation shown in Table 10.

Moreover, equations 10 – 13 were used to forecast the SIFs for double parallel surface cracks located (external or internal) on a thick cylinder under tension (TN), bending (BN), and mixed-mode loading (MX). Where (F_{TWO}) represents the normalized SIFs for two cracks, (F_{single}) denotes the normalized SIFs for a single crack, which predicts the SIFs in the case of two cracks, and (*s*) is the distance separating the flaws. Also, *a/c* and *a/t* characterize the crack geometry, while $2\Theta/\pi$ describes the location on the crack front, whilst the term t/D_i, denoted to the ratio of the cylinder thickness to the interior diameter, which is utilized to specify the cylinder as a thick cylinder, where $t/D_i > 0.05$ for the thick cylinder. It should be noted that each of the presented equations predicts the SIFs depending on the separation distance between the cracks. Similarly, equations 14 – 17 are utilized to calculate SIFs for two cracks located on a thin cylinder, where the δ represents the thin cylinder detection range; this range must be $\delta \leq 1.10$ ($\delta = D_o/D_i$) as stated by (Vullo 2014).

$$F_{TWO}f\left(\frac{a}{c},\frac{a}{t},\frac{2\theta}{\pi},\frac{t}{D_i}\right) = 0.632 \times F_{single}f\left(\frac{a}{c},\frac{a}{t},\frac{2\theta}{\pi},\frac{t}{D_i}\right) + 0.106 \quad \text{For} \quad s= \quad 3\text{mm}, \tag{10}$$

$$F_{TWO}f\left(\frac{a}{c},\frac{a}{t},\frac{2\theta}{\pi},\frac{t}{D_i}\right) = 0.634 \times F_{single}f\left(\frac{a}{c},\frac{a}{t},\frac{2\theta}{\pi},\frac{t}{D_i}\right) + 0.136 \quad \text{For} \quad s= \quad 6\text{mm}, \tag{11}$$

$$F_{TWO}f\left(\frac{a}{c},\frac{a}{t},\frac{2\theta}{\pi},\frac{t}{D_i}\right) = 0.638 \times F_{single}f\left(\frac{a}{c},\frac{a}{t},\frac{2\theta}{\pi},\frac{t}{D_i}\right) + 0.177 \quad \text{For} \quad s= \quad 12\text{mm}, \tag{12}$$

$$F_{TWO}f\left(\frac{a}{c},\frac{a}{t},\frac{2\theta}{\pi},\frac{t}{D_i}\right) = 0.718 \times F_{single}f\left(\frac{a}{c},\frac{a}{t},\frac{2\theta}{\pi},\frac{t}{D_i}\right) + 0.146 \quad \text{For} \quad s= \quad 24\text{mm}, \tag{13}$$

$$F_{TWO}f\left(\frac{a}{c},\frac{a}{t},\frac{2\theta}{\pi},\delta\right) = 0.587 \times F_{single}f\left(\frac{a}{c},\frac{a}{t},\frac{2\theta}{\pi},\delta\right) + 0.209 \quad \text{For} \quad s= \quad 3\text{mm}, \tag{14}$$

$$F_{TWO}f\left(\frac{a}{c},\frac{a}{t},\frac{2\theta}{\pi},\delta\right) = 0.579 \times F_{single}f\left(\frac{a}{c},\frac{a}{t},\frac{2\theta}{\pi},\delta\right) + 0.270 \quad \text{For} \quad s= \quad 6\text{mm}, \tag{15}$$

$$F_{TWO}f\left(\frac{a}{c},\frac{a}{t},\frac{2\theta}{\pi},\delta\right) = 0.715 \times F_{single}f\left(\frac{a}{c},\frac{a}{t},\frac{2\theta}{\pi},\delta\right) + 0.174 \quad \text{For} \quad s= \quad 12\text{mm}, \tag{16}$$

$$F_{TWO}f\left(\frac{a}{c},\frac{a}{t},\frac{2\theta}{\pi},\delta\right) = 0.928 \times F_{single}f\left(\frac{a}{c},\frac{a}{t},\frac{2\theta}{\pi},\delta\right) + 0.007 \quad \text{For} \quad s= \quad 24\text{mm}, \tag{17}$$

The obtained relationship between the SIFs of single and double cracks which is presented in the form of mathematical empirical models was tested in terms of ability and accuracy. Further, the ability is tested by the coefficient of determination (R^2), and the accuracy is examined by each of the Mean Absolute Error (MAE) and Mean Absolute

Percentage Error (MAPE). It should be noted that the same parameters have been used to evaluate the ability and accuracy of predictions in (Keprate, Ratnayake, and Sankararaman 2018; 2017). Table 10 clarifies the evaluation of the accuracy and ability of the proposed mathematical models, in terms of MAE, MAPE, and R^2. Moreover, the values of SIFs of single cracks were employed in the proposed mathematical model to determine the SIFs of two cracks, then obtained results compared to those that calculated via FEA. It must be pointed out that the proposed models were found to be appropriate to estimate SIFs for double parallel cracks located either on the outside or inside surfaces of hollow thick and thin cylinders.

Table 10. Empirical mathematical model evaluation

		Performance metrics								
		MAE			MAEP			R^2		
Eq.	***s*, mm**	**TN**	**BN**	**MX**	**TN**	**BN**	**MX**	**TN**	**BN**	**MX**
10	3	0.013	0.022	0.024	1.78	3.22	2.58	0.9993	0.9992	0.9995
11	6	0.017	0.029	0.015	2.22	4.03	1.63	0.9969	0.9963	0.9964
12	12	0.025	0.043	0.021	2.61	4.94	2.21	0.9652	0.9634	0.9707
13	24	0.046	0.040	0.041	4.50	3.48	4.03	0.9036	0.9583	0.9118
14	3	0.031	0.038	0.021	4.01	5.15	2.77	0.9633	0.9758	0.9744
15	6	0.029	0.039	0.025	3.55	4.89	3.01	0.9429	0.9378	0.9419
16	12	0.047	0.039	0.051	5.61	3.97	5.08	0.9145	0.9527	0.8771
17	24	0.044	0.032	0.052	5.67	4.76	6.52	0.8865	0.9432	0.8693

It should be emphasized that the maximum acceptable range for error between the estimated values using the empirical mathematical model and the calculated values using FEA is assumed to be less than 5% since this value is commonly used. Furthermore, MAE is the responsible parameter used to evaluate the difference between the two values, because MAE defines the direct difference (error), while MAPE describes what is the error ratio with respect to the original value. Generally, the best value of MAE is equal to zero, which means the empirical model has an accuracy of 100% in prediction. Practically, it is quite difficult to propose such a model since it depends on prediction, thus, the most satisfying results are those of MAE close to zero and should not exceed 5%. However, the maximum attained error between the calculated and estimated SIFs was equal to 0.046, which falls within the accepted range.

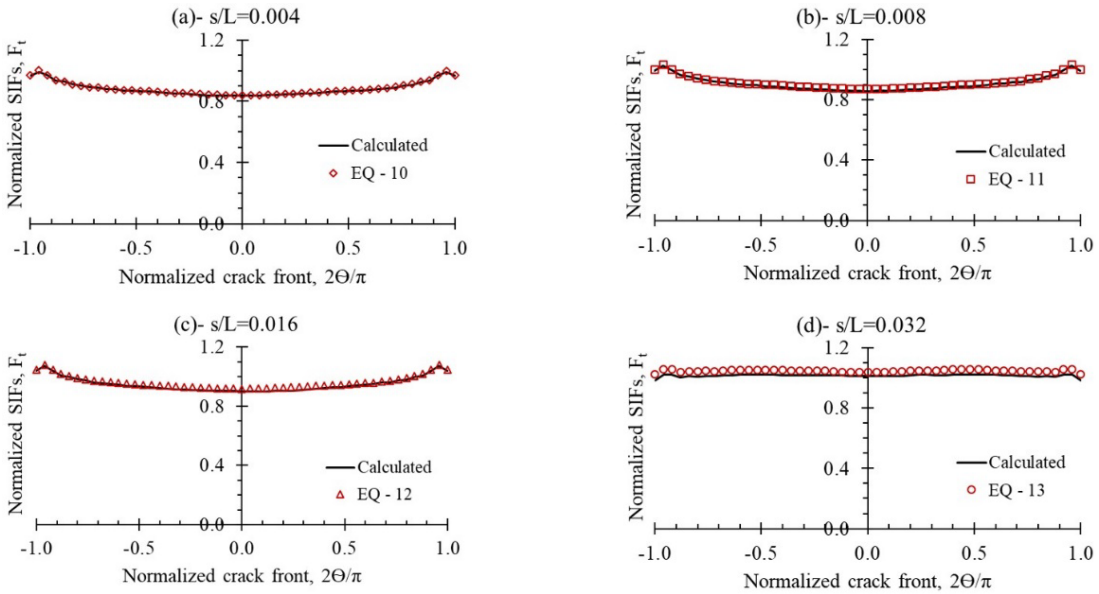

Figure 11. Validation of Equations 10 – 13 for thick cylinder under tension for a/c=0.8

Furthermore, Figures 11 and 12 depict the validation of the proposed mathematical models in terms of predicting the SIFs for double parallel cracks under tension loading. Figure 11 is dedicated to Equations 10 – 13, and Figure 12 for Equations 14 – 17, where each formula is used to predict SIFs according to the distance separating between the cracks. Based on the comparison which has been made between the calculated SIFs (the results of the current study) and the

predicted SIFs which were symbolized according to the equation number, the predicted SIFs exhibited a respectable agreement with respect to the computed SIFs. Therefore, the proposed empirical model could be used to estimate SIFs for double parallel cracks at any point on the crack front either on a thick or thin cylinder confidently.

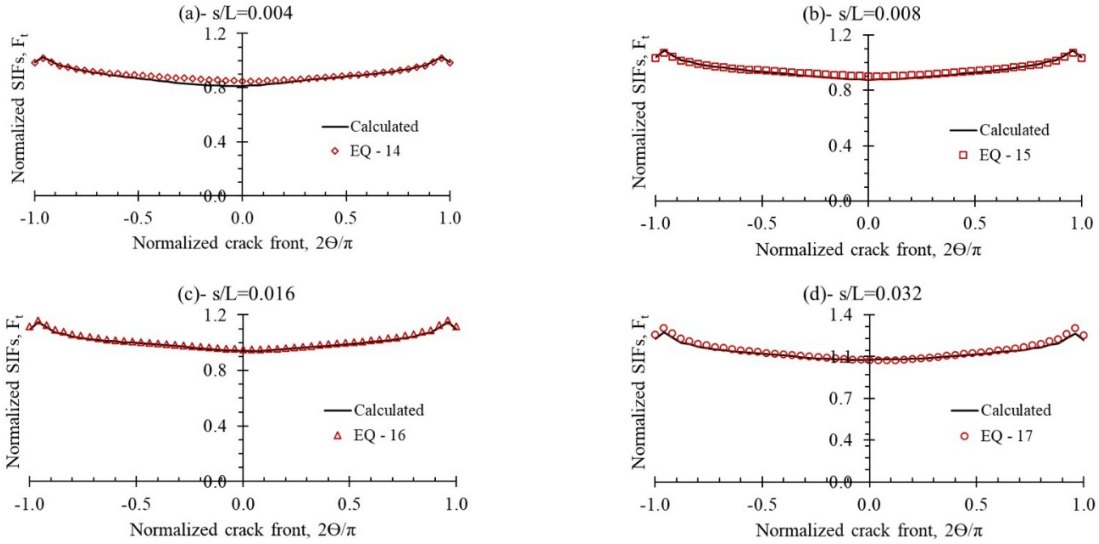

Figure 12. Validation of Equations 13 – 17 for thin cylinder under tension for a/c=0.8

5 CONCLUSIONS

The determined Stress Intensity Factor via finite element analysis for double parallel surface cracks located on thick and thin cylinders has been exploited to develop an empirical mathematical model. The developed model was applicable to estimate SIFs for cracks with an aspect ratio between 0.4 to 1.2, and relative crack depth of 0.5 and 0.8. Also, the model has the ability to predict SIFs at any point on the crack front for double cracks utilizing SIFs for single crack under each tension, bending, and mixed-mode loading. Some concluding observations could turn out to be fairly drawn as follows:

- The orientation of SIFs along the crack front for double parallel cracks was found to follow the same trend that was shown by a single crack despite the existence of crack interaction.
- The impact of interaction for double parallel cracks on SIFs is verified by only the shielding effect.
- The relative depth of the crack exhibited substantial influence on the crack interaction, where deep cracks showed high interaction rates and vice versa.
- The guideline for crack interaction criteria requires modification since the horizontal separation distance based on the API standard was found to be applicable for small crack depth only.
- For the examined types of loading, it was clear that insignificant difference between the case of the cracks if positioned on the inner or external surface. Similarly, for the same loading conditions, no significant difference has been found between the two examined types of cylinders (thick, and thin).

ACKNOWLEDGMENT

This research was supported by Universiti Tun Hussein Onn Malaysia (UTHM) through Tier 1 (vot. Q497).

Author's Contributions: Conceptualization, AE Ismail and S Jamian; Methodology, OM Al-Moayed, AK Kareem, GC Coêlho; Investigation, OM Al-Moayed, AK Kareem, GC Coêlho and AE Ismail; Writing - original draft, OM Al-Moayed, AK Kareem; Writing - review & editing, AE Ismail, S Jamian and GC Coêlho; Supervision, AE Ismail and S Jamian.

Editor: Pablo Andrés Muñoz Rojas

References

Abbaszadeh Bidokhti, Ali, and Amir Reza Shahani. 2015. "Interaction Analysis of Non-Aligned Cracks Using Extended Finite Element Method." *Latin American Journal of Solids and Structures* 12 (13): 2439–59. https://doi.org/10.1590/1679-78251664.

Al-Moayed, O M, A K Kareem, A E Ismail, S Jamian, and M N Nemah. 2019. "Distribution of Mode I Stress Intensity Factors for Single Circumferential Semi-Elliptical Crack in Thick Cylinder." *International Journal of Integrated Engineering* 11 (7): 102–11.

Al-moayed, O. M., A. K. Kareem, A. E. Ismail, S. Jamian, and M. N. Nemah. 2020. "Influence Coefficients for a Single Superficial Cracked Thick Cylinder under Torsion and Bending Moments." *International Journal of Integrated Engineering* 12 (4): 132–44.

Anis, Samsol Faizal, Motomichi Koyama, Shigeru Hamada, and Hiroshi Noguchi. 2020. "Simplified Stress Field Determination for an Inclined Crack and Interaction between Two Cracks under Tension." *Theoretical and Applied Fracture Mechanics* 107: 102561. https://doi.org/10.1016/j.tafmec.2020.102561.

"ANSYS Mechanical APDL Fracture Analysis Guide." 2019.

API, ASME. 2016. "Fitness-for-Service FFS-1 - 2016."

Awang, M K, A E Ismail, A L Mohd Tobi, and M H Zainulabidin. 2017. "Stress Intensity Factors and Interaction of Two Parallel Surface Cracks on Cylinder under Tension." In *IOP Conference Series: Materials Science and Engineering*, 165:12009.

Carpinteri, Andrea. 1993. "Shape Change of Surface Cracks in Round Bars under Cyclic Axial Loading." *International Journal of Fatigue* 15 (1): 21–26.

Coêlho, Gabriel de C, Antonio A Silva, Marco A Santos, Antonio G B Lima, and Neilor C Santos. 2019. "Stress Intensity Factor of Semielliptical Surface Crack in Internally Pressurized Hollow Cylinder—A Comparison between BS 7910 and API 579/ASME FFS-1 Solutions." *Materials* 12 (7): 1042. https://doi.org/10.3390/ma12071042.

Coêlho, Gabriel, Antonio Silva, and Marco Santos. 2022. "Elastic Surface Crack Interaction and Its Engineering Critical Assessment within the Framework of Fitness-for-Service Standards Frattura Ed Integrità Strutturale." *Frattura Ed Integrità Strutturale*.

Diamantoudis, A Th, and G N Labeas. 2005. "Stress Intensity Factors of Semi-Elliptical Surface Cracks in Pressure Vessels by Global-Local Finite Element Methodology." *Engineering Fracture Mechanics* 72 (9): 1299–1312.

Fakhri, O. M., A. K. Kareem, A. E. Ismail, S. Jamian, and Mohammed Najeh Nemah. 2019. "Mode i SIFs for Internal and External Surface Semi-Elliptical Crack Located on a Thin Cylinder." *Test Engineering and Management* 81 (11–12): 586–96.

Fakhri, Omar Mohammed. 2021. "A New Empirical Model to Predict Stress Intensity Factor for Double Interacting Surface Cracks Located in Hollow Cylinder." Thesis (Doctoral), Universiti Tun Hussein Onn Malaysia.

Franzese, Monica, and Antonella Iuliano. 2019. "Correlation Analysis." In *Encyclopedia of Bioinformatics and Computational Biology*, edited by Shoba Ranganathan, Michael Gribskov, Kenta Nakai, and Christian Schönbach, 706–21. Oxford: Academic Press. https://doi.org/10.1016/B978-0-12-809633-8.20358-0.

Gallo, Amy. 2015. "A Refresher on Regression Analysis." *Harvard Business Review* 4.

Guangwei, Meng, Guo Xuedong, Liu Hanbing, Chen Suhuan, and Wang Zhichao. 1999. "The Research of Influence Coefficients of Size on a Plate with Two Parallel Cracks." *Communications in Numerical Methods in Engineering* 15 (1): 65–73.

Guozhong, Chai, Jiang Xianfeng, Li Gan, and others. 2004. "Analyses on Interaction of Internal and External Surface Cracks in a Pressurized Cylinder by Hybrid Boundary Element Method." *International Journal of Pressure Vessels and Piping* 81 (5): 443–49.

Guozhong, Chat, Zhang Kangda, and Wu Dongdi. 1996. "Interactions of Two Coplanar Elliptical Cracks Embedded in Finite Thickness Plates under Uniform Tension." *Engineering Fracture Mechanics* 53 (2): 179–91.

Han, Zhichao, Caifu Qian, and Huifang Li. 2020. "Study of the Shielding Interactions between Double Cracks on Crack Growth Behaviors under Fatigue Loading." *Metals* 10 (2): 202.

Ismail, A. E., A. K. Ariffin, S. Abdullah, and M. J. Ghazali. 2012. "Stress Intensity Factors for Surface Cracks in Round Bar under Single and Combined Loadings." *Meccanica* 47 (5): 1141–56. https://doi.org/10.1007/s11012-011-9500-7.

Ismail, Al Emran, Saifulnizan Jamian, KamarulAzhar Kamarudin, Mohd Khir Mohd Nor, Mohd Norihan Ibrahim, and Moch. Agus Choiron. 2018. "An Overview of Fracture Mechanics with ANSYS." *International Journal of Integrated Engineering* 10 (5): 59–67. https://doi.org/10.30880/ijie.2018.10.05.010.

Jiang, Z D, J Petit, and G Bezine. 1992. “An Investigation of Stress Intensity Factors for Two Unequal Parallel Cracks in a Finite Width Plate.” *Engineering Fracture Mechanics* 42 (1): 129–38.

Kamaya, Masayuki. 2011. “A Combination Rule for Circumferential Surface Cracks on Pipe under Tension Based on Limit Load Analysis.” *Journal of Pressure Vessel Technology* 133 (2).

Keprate, Arvind, R M Chandima Ratnayake, and Shankar Sankararaman. 2017. “Comparing Different Metamodelling Approaches to Predict Stress Intensity Factor of a Semi-Elliptic Crack.” In *International Conference on Offshore Mechanics and Arctic Engineering*, 57687:V004T03A025.

Keprate, Arvind, R M Chandima Ratnayake, and Shankar Sankararaman. 2018. “Validation of Adaptive Gaussian Process Regression Model Used for SIF Prediction.” In *International Conference on Offshore Mechanics and Arctic Engineering*, 51234:V004T03A029.

Kim, D S, and K H Lo. 1995. “Crack Interaction Criteria in Pressure Vessels and Pipe.” *Journal of Offshore Mechanics and Arctic Engineering* 117 (4): 260–264.

Kirkhope, K J, R Bell, and J Kirkhope. 1991. “Stress Intensity Factors for Single and Multiple Semi-Elliptical Surface Cracks in Pressurized Thick-Walled Cylinders.” *International Journal of Pressure Vessels and Piping* 47 (2): 247–57.

Li, C. Q., and S. T. Yang. 2012. “Stress Intensity Factors for High Aspect Ratio Semi-Elliptical Internal Surface Cracks in Pipes.” *International Journal of Pressure Vessels and Piping* 96–97: 13–23. https://doi.org/10.1016/j.ijpvp.2012.05.005.

Lin, X B, and R A Smith. 1998. “Fatigue Growth Prediction of Internal Surface Cracks in Pressure Vessels.” *Journal of Pressure Vessel Technology* 120 (1): 17–23.

Marshall, Phil. 2001. *The Residual Structural Properties of Cast Iron Pipes: Structural and Design Criteria for Linings for Water Mains.* UKWIR.

Raju, I S, and J. C. Newman. 1982. “Stress-Intensity Factors for Internal and External Surface Cracks in Cylindrical Vessels.” *Journal of Pressure Vessel Technology* 104 (4): 293–98. https://doi.org/10.1115/1.3264220.

Raju, I S, and J C Newman. 1986. “Stress-Intensity Factors for Circumferential Surface Cracks in Pipes and Rods under Tension and Bending Loads.” In *Fracture Mechanics: Seventeenth Volume.* ASTM International.

Rice, James R. 1968. “A Path Independent Integral and the Approximate Analysis of Strain Concentration by Notches and Cracks.” *Journal of Applied Mechanics* 35.

Tsang, D K L, S O Oyadiji, and A Y T Leung. 2003. “Multiple Penny-Shaped Cracks Interaction in a Finite Body and Their Effect on Stress Intensity Factor.” *Engineering Fracture Mechanics* 70 (15): 2199–2214.

Vullo, Vincenzo. 2014. “Circular Cylinders and Pressure Vessels.” *Stress Analysis and Design. Springer,* Berlin.

Zhang, Y M, M Z Ariffin, Z M Xiao, W G Zhang, and Z H Huang. 2015. “Nonlinear Elastic--Plastic Stress Investigation for Two Interacting 3-D Cracks in Offshore Pipelines.” *Fatigue & Fracture of Engineering Materials & Structures* 38 (5): 540–50.

Zhang, Yanmei, Mu Fan, and Zhongmin Xiao. 2016. “Nonlinear Elastic-Plastic Stress Investigations on Two Interacting 3-D Cracks in Offshore Pipelines Subjected to Different Loadings.” *AIMS Materials Science* 3 (4): 1321–1339. https://doi.org/10.3934/matersci.2016.4.1321.